Malaysian Journal of Chemistry, 2024, Vol. 26(2), 33-45

Molecular Docking, Drug-likeness, and ADMET Predictions for Goniothalamin and its Analogues as Plasmepsin II Inhibitors

Sharinah Ideris[1,2], Syahrul Imran[1,2], Normala Abd Latip[3,4] and Che Puteh Osman[1,2*]

[1]Atta-ur-Rahman Institute for Natural Product Discovery, Universiti Teknologi MARA Cawangan Selangor, Kampus Puncak Alam, 42300 Bandar Puncak Alam, Selangor, Malaysia

[2]Faculty of Applied Sciences, Universiti Teknologi MARA, 40450 Shah Alam, Selangor, Malaysia

[3]Faculty of Pharmacy, Universiti Teknologi MARA Cawangan Selangor, Kampus Puncak Alam, 42300 Bandar Puncak Alam, Selangor, Malaysia

[4]Integrative Pharmacogenomics Institute (iPROMISE), Universiti Teknologi MARA Cawangan Selangor, Kampus Puncak Alam, 42300 Bandar Puncak Alam, Selangor, Malaysia

*Corresponding author (email: cheputeh@uitm.edu.my)

Malaria is a life-threatening disease caused by the *Plasmodium* parasite, which is transmitted to humans through the female *Anopheles* mosquito. Plasmepsin II is an essential digestive component in the parasite's food vacuole protease involved in haemoglobin degradation. Our objective was to evaluate goniothalamin and its analogues as potent antimalarial molecules with plasmepsin II inhibitory activity effective against resistant strains of *Plasmodium* parasites. A molecular docking approach was applied to identify plausible binding interactions between goniothalamin derivatives and plasmepsin II. Based on molecular docking analysis, we found that goniotriol, goniodiol, 8-acetylgoniotriol, trifluoromethyl howiinol, and parvistone formed conventional hydrogen bonds with the catalytic dyad Asp34 and Asp214 within the active site of plasmepsin II. In addition, these compounds passed the ADMET prediction test and fulfilled Lipinski's rule of five. The results of this study can be used to identify, optimize and understand goniothalamin and its analogues as potential drug candidates to accelerate the path from initial drug discovery to successful clinical application for malaria.

Keywords: Malaria; plasmepsin II; molecular docking; molecular dynamics; goniothalamin

Received: July 2023; Accepted: October 2023

Malaria continues to be a major infectious disease, with an estimated 247 million cases and 619,000 deaths annually worldwide. It was reported that 76 % of malaria deaths worldwide involved children aged under five. About 13.3 million women were exposed to malaria during pregnancy [1]. There are five parasitic species of *Plasmodium*, namely, *Plasmodium falciparum, P. vivax, P. ovale, P. malariae* and *P. knowlesi.* Among these five species, *P. falciparum* and *P. vivax* are responsible for most of the infections and deaths in human beings. Although artemisinin-based combination therapies (ACTs) have contributed to the recent success of global malaria control, the emergence of artemisinin resistance in *P. falciparum* has threatened malaria control and elimination efforts in the Greater Mekong area [2]. Resistance against artemisinin and its derivatives is characterized by a point mutation in the parasite's Kelch-like protein, a primary marker of artemisinin drugs, and is associated with increased rates of failure of ACTs in Cambodia and Thailand [3]. Chloroquine and primaquine are the mainstay treatments for malaria in most of the world. After the rise of chloroquine resistance in *P. falciparum*, sulphadoxine-pyrimethamine treatment became widespread. This has since been replaced by artesunate for the treatment of *falciparum* malaria. Antifolate drugs used against malaria include pyrimethamine, proguanil and sulfa drugs. The resistance against antifolate drugs and chloroquine is due to mutations in genes encoded for dihydrofolate reductase (DHFR) and dihydropteroate synthase (DHPS) enzymes. Many studies have also associated the resistant strains with point mutations in genes encoding for the *P. falciparum* chloroquine resistance transporter (*Pf*CRT) protein and *P. falciparum* multidrug resistance 1 (*Pf*MDR1) [4], [5]. The emergence of drug resistance is partly due to the patients' non-adherence to anti-malarial drugs [6]. In many parts of the world, parasites have developed resistance to several antimalarial drugs, so there is an urgent need to discover new antimalarial lead candidates.

The malaria parasite develops in the human host's erythrocytes, where it digests the host's haemo-globin as a source of metabolic energy and amino acids for protein synthesis [7]. The aspartic protease, called plasmepsin, has been identified during the asexual blood stage of the parasite lifecycle and has different functions [8]. Plasmepsins are categorized into ten subtypes, namely, PLM I, II, IV, V, VI, VII, VIII, IX, X, and histoaspartic protease (HAP), based on the encoding of ten different genes with high inter-

genomic similarity. Plasmepsins I, II, IV and HAP are essential digestive components in the malaria parasite's food vacuole responsible for the breakdown of haemoglobin to amino acids [9]. The plasmepsin-based antimalarials have been identified *in vitro* and *in vivo*, indicating that they are a promising new target for the discovery of new antimalarial therapies [10]. Plasmepsin II attracted the most attention due to its early discovery as a starting point for developing novel protease inhibitors, and its ease of production in large quantities using *Escherichia coli* (*E. coli*) [11-12]. The molecular structure of plasmepsin II consists of three distinct regions, the *N*-terminal domain, the C-terminal domain and a 6-β-sheet domain that connects these two lobes. The active site of plasmepsin II is located at the N-terminal and C-terminal domain contacts and contains two aspartic acid residues (Asp34 and Asp214), a proton donor and acceptor, forming a catalytic dyad during cleavage of the peptide bond [13]. Plasmepsin II displays only 30 - 35 % similarity to human aspartic proteases such as pepsin, renin, gastricsin, cathepsin D, and cathepsin E [14]. The protein inhibitor interactions observed between plasmepsin II and human renin indicate a different binding mode and degree of flexibility in the active site [8].

The genus *Goniothalamus* consists of 160 species distributed throughout the tropical forests of Southeast Asia, some of which are widely used in folk medicine [15]. Styryl lactones are a group of secondary metabolites that have been reported mainly within this genus. The naturally occurring styryl lactone goniothalamin **1** was first isolated from the dried bark of *Cryptocarya caloneura* in 1967 (**Figure 1**). It was later isolated from various *Goniothalamus* species [16]. Goniothalamin **1** and its analogues represent natural and synthetic chemicals that have been demonstrated to possess an interesting variety of biological activities [17]. Many researchers developed an interest in producing synthetic derivatives of goniothalamin **1** due to its potent activity against various diseases. Recent studies showed that **1** displayed antimalarial activity through the *P. falciparum* lactate dehydrogenase (*Pf*LDH) assay. In addition, the combination of **1** and chloroquine was shown to improve parasitemia reduction and prolong the survival of treated mice [18]. Structure-activity relationship (SAR) studies of goniothalamin **1** showed that the Michael acceptor sub-unit in the lactone ring, the *trans*-oriented double bond in the linker part, and the configuration of the stereogenic centre carbon are responsible for its biological activity [19].

In this study, molecular docking was used to evaluate the binding energies and interactions of goniothalamin **1** and its analogues against potential therapeutic drug targets such as plasmepsin II. The potential inhibitors were selected based on their interactions with active site residues. The selected compounds were subjected to further analyses which included physicochemical characterization, bioactivity scoring, absorption, distribution, metabolism, excretion and toxicity. The results showed that the selected compounds exhibited promising antimalarial activity, which is a crucial consideration for drug design and development.

EXPERIMENTAL

Ligand Preparation

Goniothalamin **1** and twenty-nine (29) analogue structures were obtained from a literature review and the PubChem Compound database (http://pubchem.ncbi.nlm.nih.gov/) (**Figure 2**). The 3D structures of these ligands were created with Chem3D Ultra 8.0 software, and energy was minimized using the MMFF94 force field.

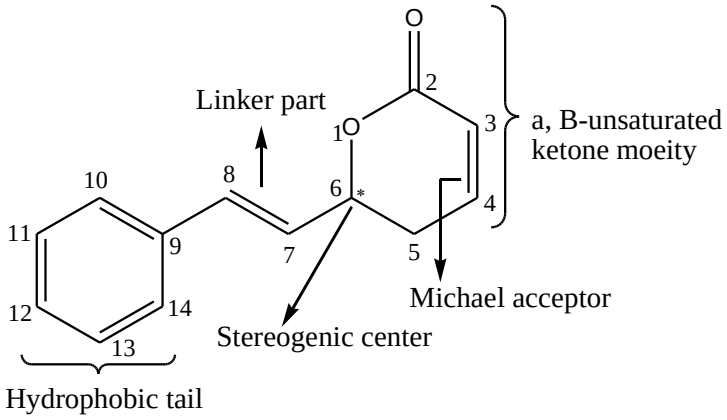

Figure 1. Sources of biological activity in the structure of goniothalamin **1**.

Preparation of Protein

The X-ray crystal structure of the plasmepsin II protein (PDB ID: 1LF3) [20] was obtained from the Protein Data Bank (www.rscb.org). This structure was chosen because of its slightly larger substrate-binding site at the subfragment-1 (S'_1) subpocket, which can accommodate a larger heterocyclic group in the P1' position of EH58 [21]. The catalytic dyad of Asp214 and Asp34, one of which was protonated while the other was negatively charged, was modelled according to a previous molecular dynamic study [21]. Protein files (PDB) were further optimized by removing bound ligands and water molecules. During preparation, hydrogen atoms and Kollman charges were added to the proteins.

Molecular Docking

Molecular docking studies were carried out using AutoDock 4.2 software. Configuration files were created for the proteins by setting suitable Cartesian coordinates to generate the grid box. The active grid was generated for docking with 40 x 42 x 40 along with x, y and z coordinates of 16.215, 6.85 and 27.605, respectively, with a grid spacing of 0.375 Å. The docking study was performed using the Lamarckian-Genetic Algorithm (LGA) method with default parameters, and docking runs were set at 150 conformations per ligand.

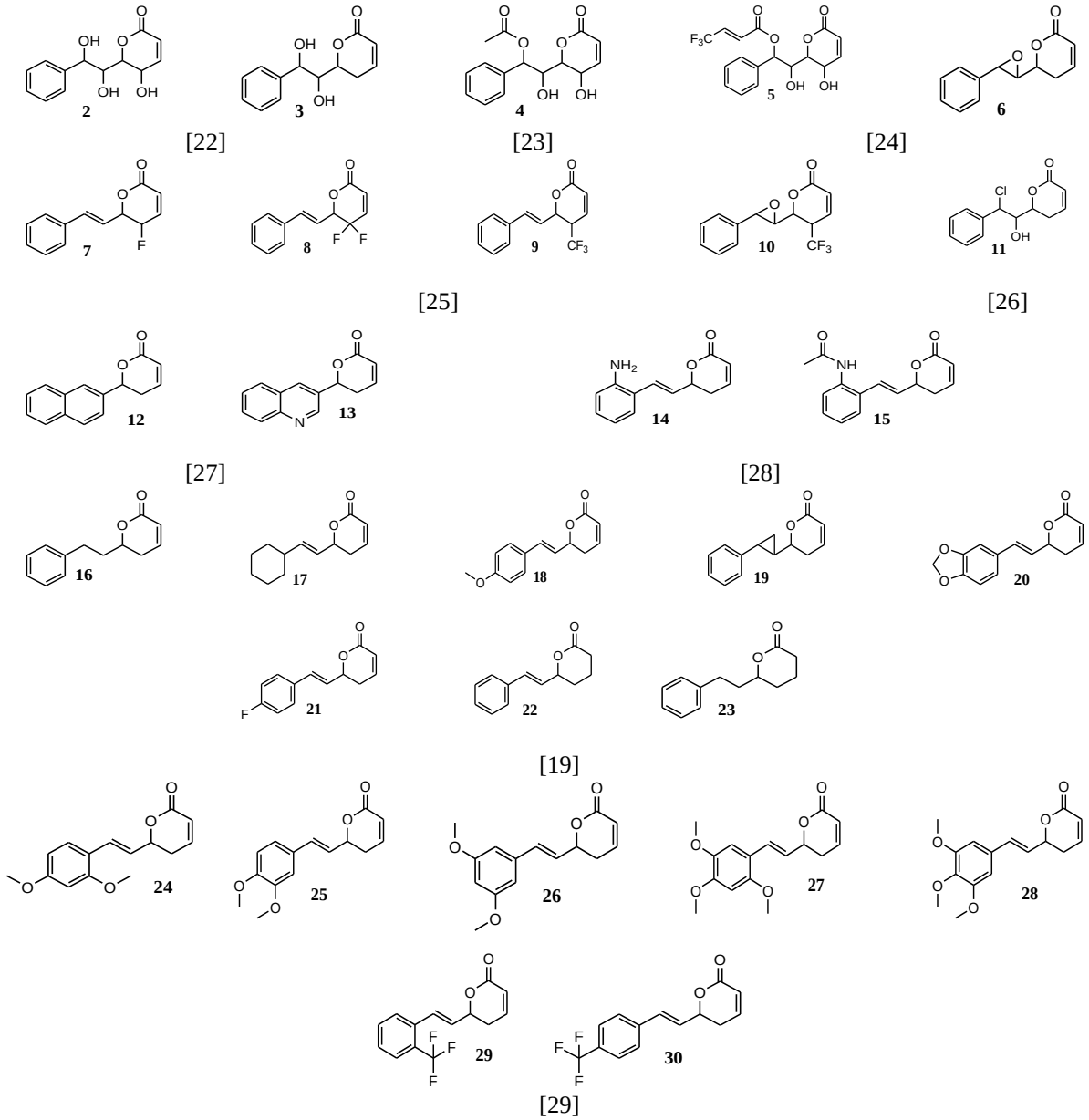

Figure 2. Chemical structures of ligands used in the molecular docking study.

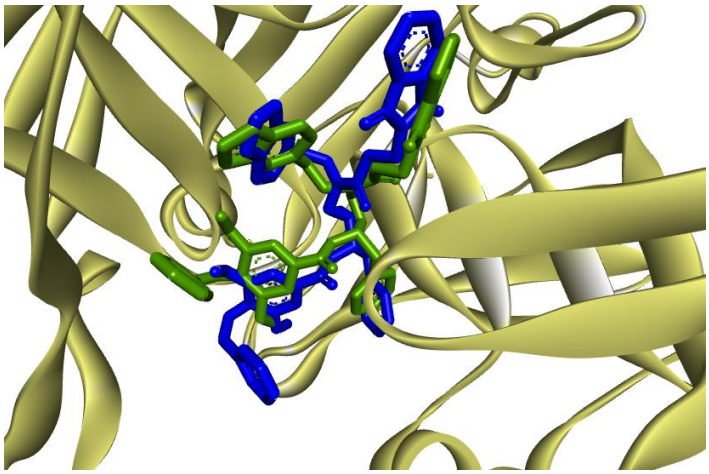

Figure 3. Re-docking pose (blue = original, green = docked).

Toxicity Prediction

The mutagenicity, tumorigenicity, irritant and reproductive effects of the compounds were calculated using the Osiris toxicity predictor (https://www.organic-chemistry.org/prog/peo/) and the toxicity results for each compound were compared with the standard drugs.

Physicochemical Properties

The physicochemical properties of the compounds were predicted using the Molinspiration molecular properties calculator (https://www.molinspiration.com/). Lipinski's rule of five analysis predicts that good absorption or permeation is more likely observed when there are less than 5 H-bond donors (<5), 10 H-bond acceptors (<10), the molecular weight is < 500 g/mol, log P of less than 5, the polar surface area (PSA) of a molecule is less than <140 $Å^2$ and the rotatable bonds (RB) count is less than 10 [30]. Hence, compounds will likely become more orally bioavailable as a drug if their properties fall within these boundaries.

Bioactivity Scores

The bioactivity score of a compound was predicted by calculating the activity score for the G-protein coupled receptor (GPCR) ligand, ion channel modulator, kinase inhibitor and nuclear receptor ligand. All parameters were predicted using the Molinspiration drug-likeness score (https://www.molinspiration.com/) [31]. The drug-likeness score was calculated and compared with the specific activity of each compound.

***In Silico* Pharmacokinetic Profile (ADME)**

The pharmacokinetic profile i.e., absorption, distribution, metabolism and excretion of the selected ligands were examined to determine their activity within the human body. The ADME characteristics of the ligands were assessed using pkCSM [32] and SWISSADME [33]. The compound's structure SMILE was retrieved from the PubChem Compound database and used as the input file for the pkCSM and SWISSADME online tools.

RESULTS AND DISCUSSION

Validation of Docking Study

A validation of the docking of the native ligand EH58 on the structure 1LF3 was run to ensure the accuracy and performance of the results obtained. The root mean square deviation (RMSD) value obtained from the re-docking of the co-crystallized ligand EH58 against 1LF3 (**Figure 3**) was 1.83 Å, which suggests the accuracy of the docking method was acceptable. For successful validation of the docking method, the RMSD value should not be more than 2.0 Å [34-35].

Binding Energies (kcal/mol)

As shown in **Table 1**, the binding energies of the docked compounds towards 1LF3 ranged between -7.20 kcal/mol and -5.65 kcal/mol. The corresponding binding energies of all compounds showed a negative value demonstrating that all compounds were able to dock in the binding pocket of the protein. The binding energy obtained through docking was due to the interactions of the compound with the protein through van der Waals, hydrogen bonding, electrostatic and intermolecular interactions, desolvation energy and torsion energy. Among the compounds, 10-acetylamino-*goniothalamin*, **15** showed the highest binding energy of -7.14 kcal/mol. However, ligand **15** did not interact with the catalytic dyad Asp34 and Asp214 of the target receptor 1LF3.

Table 1. The binding energies (kcal/mol) and hydrogen bond interaction residues of all studied compounds and standard drugs at the active site of 1LF3.

Compound	Binding energy (Kcal/mol)	Hydrogen bond interacting residues
1	-6.46	Ser79, Val78
2	-5.86	Asp34, Ser79, Tyr192, Val78
3	-5.70	Asp34, Ser79, Val78
4	-6.63	Asp34, Ser79, Tyr192, Val78
5	-6.51	Asp214, Ser79, Val78
6	-6.19	Ser79, Val78
7	-6.16	Ser79, Val78
8	-5.93	Ser79
9	-6.05	Ser79, Thr217
10	-6.18	Ser79, Tyr192, Val78
11	-6.80	Asp34, Ser79, Val78
12	-6.42	Ser79, Val78
13	-6.78	Ser79, Tyr192, Val78
14	-6.26	Asn76, Ser79, Val78
15	-7.14	Ser79, Tyr192, Val78
16	-6.18	Ser79, Val78
17	-6.42	Val78
18	-5.83	Ser79, Val78
19	-6.18	Ser79, Val78
20	-6.33	Ser79, Val78
21	-6.07	Ser79, Val78
22	-6.30	Ser79, Val78
23	-6.19	Ser79, Val78
24	-6.33	Ser79, Tyr192, Val78
25	-5.92	Ser79, Tyr192
26	-6.23	Ser218, Thr217, Tyr192, Val78
27	-5.83	Ser79, Tyr192
28	-6.01	Ser79, Tyr192
29	-6.14	Ser79, Tyr192, Val78
30	-5.65	Ser79, Val78
Chloroquine	-7.20	Asp34, Tyr192
Pyrimethamine	-6.65	Asp34, Asp214, Gly216

Molecular Docking Analysis

Table 1 shows the hydrogen bond interactions of thirty ligands and standard drugs with the residues of 1LF3. Most of the compounds exhibited interactions with the flap residues Val78 and Ser79, the catalytic dyad Asp34 and Asp214, and the residues Tyr192 and Thr217 that were adjacent to the catalytic dyad. Potential inhibitors in this study were selected based on their interactions with the catalytic dyad present within the binding active site of the protein [36]. These interactions may increase biological activity.

Figures 4 and **5** illustrate the 2D and 3D-binding sites between compounds **1**, **2**, **3**, **4**, **5** and **11**, and the target protein plasmepsin II. In the molecular docking study, goniothalamin **1** was found to bind to 1LF3 through hydrogen bonds, hydrophobic forces, π-sulfur and van der Waals bonds. The results of the docking study showed that **1** exhibited a binding energy of -6.46 kcal/mol. Four potential conventional hydrogen bonds were observed between the two oxygen atoms of **1** with Val78 (3.08 Å and 3.07 Å) and Ser79 (3.04 Å and 2.77 Å), respectively. The aromatic ring of **1** formed π-alkyl and π-sulfur interactions with Ile131 and Met15 at distances of 4.73 Å and 5.94 Å, respectively. Compound **1** did not form any conventional hydrogen bond with the catalytic dyad residues of Asp34 and Asp214. Therefore, modifications to the structure of **1** are needed to introduce additional binding interactions with the active site residues of plasmepsin II.

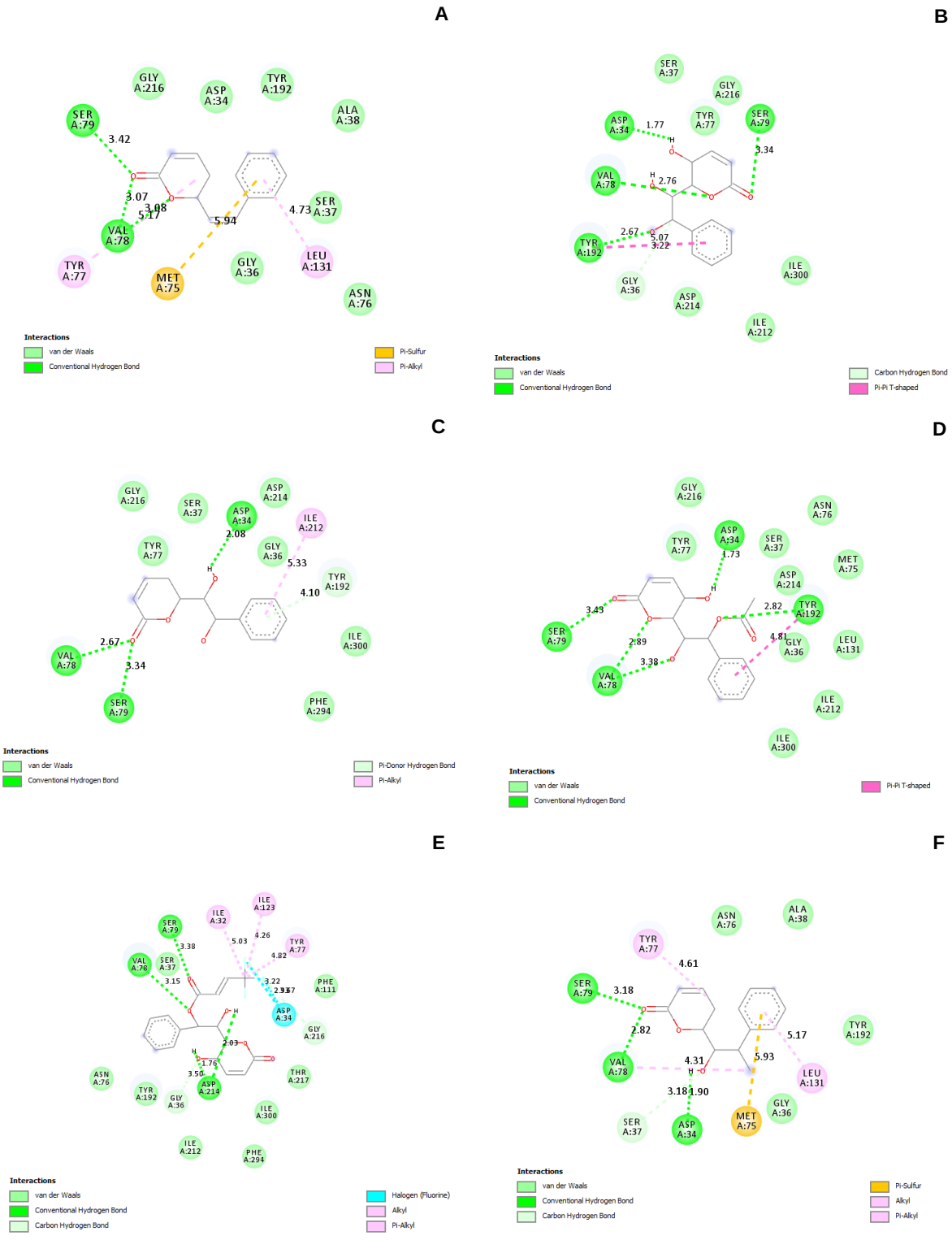

Figure 4. 2D binding sites of A) goniothalamin **1**, B) goniotriol **2**, C) goniodiol **3**, D) 8-acetylgoniotriol **4**, E) trifluoromethyl howiinol **5,** F) parvistone **11**, in the binding pocket of the plasmepsin II receptor.

Five analogues of goniothalamin **2**, **3**, **4**, **5** and **11** interacted with the catalytic dyad Asp34 or Asp214 through conventional hydrogen bonds. Conventional hydrogen bonds are stronger interactions that may lead to the stability of the protein structure, and selectivity of protein-ligand interactions [37]. The five compounds exhibited an average of four hydrogen bonds with optimum bond distances ranging between 1.73 to 2.08 Å. This result is also in line with Lipinski's rule of five criteria of not more than five hydrogen bond donors and ten hydrogen bond acceptors for oral bioavailability.

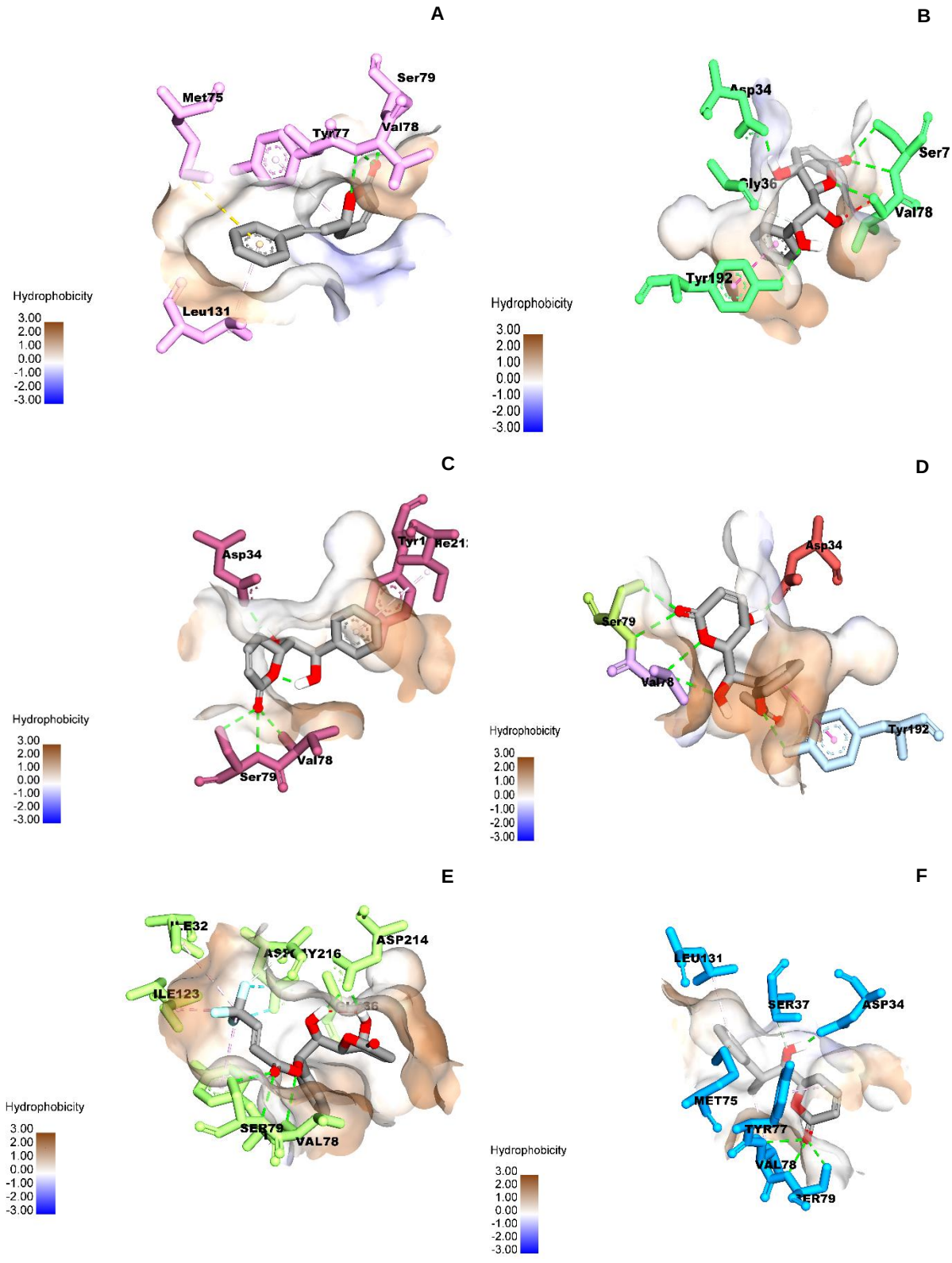

Figure 5. 3D binding sites of A) goniothalamin **1**, B) goniotriol **2,** C) goniodiol **3,** D) 8-acetylgoniotriol **4,** E) trifluoromethyl howiinol **5,** F) parvistone **11**, between the target proteins.

Goniotriol **2** was found to possess a binding energy of -5.86 kcal/mol. The docking study showed that the hydroxyl on lactone ring C5 of **2** was able to form a conventional hydrogen bond with Asp34 at 1.77 Å. This hydrogen bond prevents the substrate of plasmepsin II from attacking the Phe33-Leu34 peptide bond of the α-chain in the host haemoglobin. The inhibition of Asp34 by **2** may cause the haemoglobin degradation process to be hindered. Two conventional hydrogen bonds were observed between the oxygen

atoms on the lactone ring with the hydrogen atoms of flap residues Val78 and Ser79 at distances of 2.76 Å and 3.34 Å, respectively. Additionally, the presence of hydroxyl groups at the linker part of **2** may lead to the formation of a conventional hydrogen bond interaction with Tyr192 at 2.67 Å. A carbon-hydrogen bond was observed between the carbon atom at the linker part and the oxygen of Gly36 at 3.22 Å, in proximity to the catalytic dyad. The aromatic ring of compound **2** formed a π-π T-shaped interaction with the π orbital of Tyr192 at 5.07 Å.

Goniodiol **3**, with a binding energy of -5.70 kcal/mol, formed conventional hydrogen bonds through the hydroxyl group at the linker part and active site residue Asp34 at a distance of 2.08 Å. Two conventional hydrogen bonds were observed between the oxygen atom of the lactone ring with Val78 and Ser79 at distances of 2.67 Å and 3.33 Å, respectively. The aromatic ring in **3** formed π-alkyl interactions with Ile212 at a distance of 5.33 Å. Further, the aromatic ring formed pi-donor hydrogen bond interactions with the hydroxyl group of Tyr92 at a distance of 4.10 Å.

8-acetylgoniotriol **4** displayed a binding energy of -6.63 kcal/mol with interactions similar to compound **2**. The replacement of hydrogen with hydroxyl on lactone ring C5 allowed the formation of a conventional hydrogen bond with Asp34 at a distance of 1.73 Å. Two conventional hydrogen bonds could potentially form between the oxygen atoms on the lactone ring with the hydrogen of Val78 and Ser79 at distances of 2.89 Å and 3.43 Å, respectively. Two conventional hydrogen bonds were also observed between oxygen atoms at the linker part of **4** with Tyr192 (2.82 Å) and Val78 (3.38 Å). The π-π T-shaped interaction was observed between the aromatic ring and π orbital of Tyr192 at a distance of 4.81 Å.

Trifluoromethyl howiinol **5**, with a binding energy of -6.51 kcal/mol, formed two conventional hydrogen bonds and two halogen bonds with the active site of the protein. The presence of the hydroxyl group at C5 and the linker part in the structure of **5** could lead to the formation of two hydrogen bond interactions with the oxygen of Asp214 at distances of 1.76 Å and 2.03 Å, respectively. Additionally, the ester group on the linker part of **5** interacted with the hydrogen atoms of Val78 (3.15 Å) and Ser79 (3.38 Å) through conventional hydrogen bonds. Compound **5** could potentially form two halogen bonds with the active site residue Asp214 (3.22 Å, 2.93 Å). Hydrophobic interactions were observed between alkyl groups of compound **5** with Ile32 (5.23Å) and Ile123 (4.26Å). A hydrophobic interaction was also observed between the alkyl part of **5** and the aromatic ring of Tyr77 at a distance of 4.82 Å.

Parvistone **11** was found to possess a binding energy of -6.80 kcal/mol. The hydrogen of the hydroxyl group on the linker part of **11** formed hydrogen bonds with the active site residue Asp34 at a distance of 1.90 Å. A carbon-hydrogen bond was observed between the carbon atom on the linker part and the carbon of Ser37 at 3.18 Å. Two conventional hydrogen bonds were observed between oxygen atoms of the lactone ring and hydrogen atoms of Ser79 (3.18 Å) and Val78 (2.82 Å). A hydrophobic interaction was observed between chlorine atoms on the linker part of **11** and the alkyl part of Val78 at 4.31 Å. A π-sulfur bond was observed between the π orbital of the aromatic ring and sulfur of Met75 at 5.93 Å. A π alkyl interaction was also observed between the π-orbital of the aromatic ring and the alkyl group of Ile131 (5.17 Å).

Toxicity Properties and Drug-likeness Analysis

Drug-likeness, derived from structural features and various molecular properties, has been widely used to determine whether a particular molecule is similar to an existing drug such as chloroquine and pyrimethamine. The results of the toxicity risk predictor indicate potential risks. The mutagenicity, tumorigenicity, irritant and reproductive effects of the compounds are indicated by bullet codes (**Table 2**). Compounds with high risks and undesired effects are indicated by white circles. A square indicates a slight risk, while a black circle indicates drug-conforming behaviour. From the data in **Table 2,** compounds **1**, **2**, **3** and **5** showed non-mutagenicity, non-tumorigenicity, and non-irritant effects, with no reproductive system toxicity compared to standard drugs. However, compound **4** showed a slight risk of irritant effects. Compound **11** was highly mutagenic, with irritant and reproductive effects but had drug-conforming tumorigenic behaviour. It has been shown that for compounds to have a reasonable probability of being well absorbed, their log P value must not be greater than 5.0. From the data evaluated in **Table 2**, all the compounds were predicted to have log P values of less than 5. More than 80 % of marketed drugs have an estimated solubility value greater than -4. The solubilities of the compounds in this study were in the range of -1.45 and -3.11. The drug-likeness of these compounds was almost comparable with that of the standard drugs, as shown in **Table 2**. The drug score combines drug-likeness, C log P, solubility, molecular weight, and toxicity risks in one handy value that can be used to judge the compound's overall potential to qualify for a drug. Compound **2** possessed the highest drug score but compound **11** had a slightly lower score than the standard drugs. On the other hand, compounds **2**, **3**, **4** and **5** were found to have higher drug score values than the standard drugs.

Table 2. Toxicity risks and drug likeness of the selected compounds.

Compound	Toxicity risks[a]				Bioavailability and drug score properties[b]			
	MUT	TUM	IRRIT	RE	CLP	S	DL	DS
1	●[d]	●	●	●	2.14	-2.93	-4.81	0.46
2	●	●	●	●	-0.68	-1.45	-2.83	0.51
3	●	●	●	●	0.18	-1.85	-3.79	0.49
4	●	●	□[e]	●	-0.19	-1.86	-2.10	0.42
5	●	●	●	●	0.85	-3.11	-9.85	0.43
11	○[c]	●	○	○	1.80	-2.79	-5.57	0.10
Pyrimethamine	○	●	○	○	2.54	-4.91	-0.24	0.11
Chloroquine	○[c]	●	○	●	4.01	-4.06	7.39	0.25

a MUT: mutagenic; TUM: tumourigenic; IRRIT: irritant; RE: reproductive effects.
b CLP: C log P; S: Solubility; DL: drug likeness; DS: drug score.
c ○: high risks and undesired effects; d ●: slight risk: e □: drug-conforming behaviour.

Table 3. Physicochemical properties of selected compounds.

Compound	miLog P	TPSA	natoms	MW	nON	nOHNH	nViolations	nRotb	Volume
1	3.16	26.30	15	200.24	2	0	0	2	189.63
2	0.07	86.99	18	250.25	5	3	0	3	219.95
3	0.98	66.76	17	234.25	4	2	0	3	211.91
4	0.91	93.07	21	292.29	6	2	0	5	256.46
5	2.14	93.07	26	372.30	6	2	0	7	298.62
11	2.36	46.53	17	252.70	3	1	0	3	217.43

Note: miLogP: logarithm of compound partition coefficient between n-octanol and water; TPSA: topological polar surface area; MW: molecular weight; nON: number of hydrogen bond acceptors; nOHNH: number of hydrogen bond donors; nViolations: number of violations; nRotb: number of rotatable bonds.

Analysis of Physicochemical Properties

Molinspiration tools were used to analyse the physicochemical properties of the compounds based on Lipinski's rule of five. According to this rule, a good drug candidate has the following characteristics: molecular weight ≤ 500 g/mol, log P ≤ 5, number of hydrogen bond acceptors ≤ 10, and number of hydrogen bond donors ≤ 5. Our results show that all the selected compounds obeyed Lipinski's rule of five **(Table 3)**. Lipophilicity (mi log P) is an important parameter which influences the oral availability of compounds. The mi log P values were below five for all the selected compounds, especially compound **2**, suggesting that they have good lipophilicity. The topological polar surface area (TPSA) value helps predict the solubility of a drug through its hydrogen bonding potential involving polar nitrogen and hydrogen atoms in the molecule. The compounds were all found to have less than 140 $Å^2$ of TPSA, suggesting good solubility. Compounds with low TPSA values can easily penetrate the blood-brain barrier and gastrointestinal barrier. Other parameters include the number of atoms (natoms), the number of rotatable bonds (nRotb), and molecular volume (volume) defining the molecular conformational flexibility. The acceptable ranges for these parameters are: natoms = 20–70, nRotb < 10, and volume < 500. As indicated in Table 3, all compounds had nRotb and volume values within the acceptable ranges. The natoms of compounds **4** and **5** were also acceptable.

Bioactivity Scores

The bioactivity of the studied compounds was predicted using Molinspiration software, which provides a bioactivity score of the compound against regular human receptors such as G protein-coupled receptor (GPCR) ligands, ion channel modulators, kinase, nuclear receptor ligands, proteases, and enzymes. The bioactivity scores of all the studied compounds are presented in **Table 4**. Generally, a compound having a high bioactivity score will have high biological activity. A compound having a bioactivity score of more than 0.00 indicates higher activity, while compounds with values between -0.50 and 0.00 are moderately active, and compounds with values less than -0.50 are inactive. As indicated in Table 4, all compounds showed remarkable biological properties and should produce good physiological action by interacting with GPCR ligands, ion channel modulators and other enzymes. The bioactivity score for GPCR ligand activity was between 0.06 and 0.20 suggesting potential activity, but compound **1** was moderately active toward the target drug. The bioactivity scores for ion channel modulator activity were between -0.04 and 0.24, suggesting strong interactions

with the target drug. Bioactivity scores for kinase inhibition modular activity were between -0.62 and -0.04. Only compound **1** showed a score of less than -0.50 suggesting inactivity towards the target drug. Bioactivity scores for nuclear receptor ligands and protease inhibitors were observed to be in the range of -0.24 to 0.30 and -0.47 to 0.20, respectively, suggesting potential activity toward the target drugs. The score for enzyme inhibitor activity was between 0.40 and 0.58 suggesting potential activity toward the target drug. The most promising compounds were **3** and **4**, based on their bioactivity scores against GPCR ligands, ion channel modulators, nuclear receptor ligands, proteases, and enzymes, respectively.

Table 4. Bioactivity scores[a] of all the selected compounds.

Compound	GPCRL	ICM	KI	NRL	PI	EI
1	-0.18	0.02	-0.62	-0.24	-0.47	0.43
2	0.06	-0.04	-0.44	0.19	-0.07	0.48
3	0.14	0.23	-0.29	0.27	0.15	0.58
4	0.14	0.00	-0.39	0.24	0.12	0.46
5	0.15	-0.01	-0.27	0.30	0.20	0.41
11	0.20	0.24	-0.04	-0.09	-0.05	0.40

[a] GPCRL: GPCR ligand; ICM: ion channel modulator; KI: kinase inhibitor; NRL: nuclear receptor ligand; PI: protease inhibitor; EI: enzyme inhibitor

Table 5. Predicted ADME values of the selected compounds.

Compound	1	2	3	4	5	11	Chloroquine	Pyrimethamine
Absorption								
TPSA	26.30	86.99	66.76	93.06	93.06	46.53	28.16	77.82
Water solubility (log S)	-2.591	-1.714	-1.522	-2.090	-3.648	-2.263	-4.117	-2.960
Caco2 permeability	1.673	0.431	0.469	0.408	0.391	1.292	1.263	1.157
Human intestinal absorption (% absorbed)	97.12	64.42	68.24	68.102	67.69	94.03	89.69	92.35
Skin Permeability	-1.914	-3.485	-3.140	-2.873	-3.264	-2.435	-2.704	-2.846
P-glycoprotein substrate (yes/no)	No	No	No	No	No	No	Yes	No
Distribution								
VDss (human)	0.261	-0.134	-0.162	-0.469	-0.499	0.082	1.528	-0.201
Fraction unbound (human)	0.254	0.488	0.390	0.322	0.314	0.319	0.280	0.278
BBB permeability	0.190	-0.690	-0.207	-0.101	-0.568	0.232	0.423	0.188
Metabolism								
CYP1A2 (inhibitor) (yes/no)	Yes	No	No	No	No	No	No	Yes
CYP2C19 (inhibitor) (yes/no)	No	No	No	No	No	No	No	No
CYP2C9 (inhibitor) (yes/no)	No	No	No	No	No	No	No	No
CYP2D6 (inhibitor)	No	No	No	No	No	No	No	Yes

(yes/no)								
CYP3A4 (inhibitor) (yes/no)	No	No	No	No	No	No	No	No
Excretion								
Total clearance	0.783	0.515	0.669	0.548	0.380	0.338	1.056	-0.031
Renal OCT2 substrate	No	No	No	No	No	No	No	No

ADME Parameters (pharmacokinetics) Analysis

Pharmacokinetic profile assessment, such as absorption, distribution, metabolism, and excretion (ADME) analysis, is very crucial in the early stage of drug discovery to minimize the lack of efficacy and identify unacceptable side effects of potential compounds. The ADME parameters of compounds and the standard drugs (chloroquine and pyrimethamine) were assessed using Swiss ADME and pkCSM. The results are presented in **Table 5**. Compounds **1** and **11** were predicted to have higher Caco-2 permeability than chloroquine and pyrimethamine. All compounds displayed high absorption characteristics, with absorption rates between 64.42 % to 97.12 %, especially compound **1**. Compounds **2**, **3** and **5** had higher skin permeability than standard drugs. All the compounds and pyrimethamine were found to be non-substrates of glycoprotein. The volume of distribution (VDss) values of compounds **2**, **3**, **4**, **5** and pyrimethamine were low, whereas compounds **1**, **11** and chloroquine had moderate values. All the compounds and standard drugs could readily cross the blood-brain barrier (BBB). We have also investigated whether the compounds and standard drugs are likely to be cytochrome P450 inhibitors. Compound **1** and pyrimethamine were predicted as potential inhibitors of the CYP1A2 enzyme. All the compounds and standard drugs were found as substrates for renal uptake transporters in the proximal convoluted tubule (OCT2).

CONCLUSION

Five potential inhibitors of plasmepsin II were identified through docking analysis. The results showed that compounds **2**, **3**, **4**, **5** and **11** had negative binding energies and interacted with the catalytic dyad Asp34 and Asp214. These compounds passed Lipinski's rule of five test, and showed potential through ADMET analysis. In addition, compounds **2**, **3** and **5** had the highest drug-likeness scores, respectively. However, *in vitro* or *in vivo* studies of the identified compounds as potential antimalarial drugs are warranted in the future.

ACKNOWLEDGEMENTS

The authors would like to acknowledge Universiti Teknologi MARA and Atta-ur-Rahman Institute for Natural Product Discovery (AuRIns) for providing designated labs and facilities for the research. Syahrul Imran would like to thank Universiti Teknologi MARA for the financial support under the Young Talent Researcher (YTR) grant file No. 600-RMC/YTR/5/3 (008/2021).

REFERENCES

1. WHO (2022) World Malaria Report 2022. Available at.https://www.who.int/teams/global-malaria-programme/reports/world-malaria-report-2022.

2. WHO (2018) World Malaria Report 2018. Available at https://www.who.int/teams/global-malaria-programme/reports/world-malaria-report-2018.

3. Tun, K. M., Imwong, M., Lwin, K. M., Win, A. A., Hlaing, T. M., Hlaing, T. and Woodrow, C. J. (2015) Spread of artemisinin-resistant Plasmodium falciparum in Myanmar: A cross-sectional survey of the K13 molecular marker. *The Lancet Infectious Diseases*, **15(4)**, 415–421.

4. Plowe, C. V., Kublin, J. G. and Doumbo, O. K. (1998) P. falciparum dihydrofolate reductase and dihydropteroate synthase mutations: epidemiology and role in clinical resistance to antifolates. *Drug Resistance Updates*, **1(6)**, 389–396.

5. Fidock, D. A., Nomura, T., Talley, A. K., Cooper, R. A., Dzekunov, S. M., Ferdig, M. T. and Wellems, T. E. (2000) Mutations in the P. falciparum digestive vacuole transmembrane protein PfCRT and evidence for their role in chloroquine resistance. *Molecular Cell*, **6(4)**, 861–871.

6. Bruxvoort, K., Goodman, C., Patrick Kachur, S. and Schellenberg, D. (2014) How patients take malaria treatment: A systematic review of the literature on adherence to antimalarial drugs. *PLoS ONE*, **9(1)**.

7. MacKintosh, C. L., Beeson, J. G. and Marsh, K. (2004) Clinical features and pathogenesis of severe malaria. *Trends in Parasitology*, **20(12)**, 597–603.

8. Silva, A. M., Lee, A. Y., Gulnik, S. V., Majer, P., Collins, J., Bhat, T. N. and Erickson, J. W. (1996) Structure and inhibition of plasmepsin II, a haemoglobin-degrading enzyme from Plasmodium

falciparum. *Proceedings of the National Academy of Sciences of the United States of America*, **93(19)**, 10034–10039.

9. Dan, N. and Bhakat, S. (2015) New paradigm of an old target: An update on structural biology and current progress in drug design towards plasmepsin II. *European Journal of Medicinal Chemistry*, **95**, 324–348.

10. Miller III, W. A., Teye, J., Achieng, A. O., Mogire, R. M., Akala, H., Ong'echa, J. M. and Kwofie, S. K. (2018) Antimalarials: Review of Plasmepsins as Drug Targets and HIV Protease Inhibitors Interactions. *Current Topics in Medicinal Chemistry*, **18(23)**, 2022–2028.

11. Francis, S. E., Gluzman, I. Y., Oksman, A., Knickerbocker, A., Mueller, R., Bryant, M. L. and Goldberg, D. E. (1994) Molecular characterization and inhibition of a Plasmodium falciparum aspartic haemoglobinase. *EMBO Journal*, **13(2)**, 306–317.

12. Hill, J., Tyas, L., Phylip, L. H., Kay, J., Dunn, B. M. and Berry, C. (1994) High level expression and characterisation of Plasmepsin II, an aspartic proteinase from Plasmodium falciparum. *FEBS Letters*, **352(2)**, 155–158.

13. Karubiu, W., Bhakat, S., McGillewie, L. and Soliman, M. E. S. (2015) Flap dynamics of plasmepsin proteases: Insight into proposed parameters and molecular dynamics. *Molecular BioSystems*, **11(4)**, 1061–1066.

14. Subramanian, E., Swan, I. D. A., Liu, M., Davies, D. R., Jenkins, J. A., Tickle, I. J. and Blundell, T. L. (1977) Homology among acid proteases: Comparison of crystal structures at 3Å resolution of acid proteases from Rhizopus chinensis and Endothia parasitica. *Proceedings of the National Academy of Sciences of the United States of America*, **74(2)**, 556–559.

15. Wiart, C. (2007) *Goniothalamus* Species : A Source of Drugs for the Treatment of Cancers and Bacterial Infections? *Hindawi*, **4**, 299–311.

16. Weber, A., Döhl, K., Sachs, J., Nordschild, A. C. M., Schröder, D., Kulik, A. and Pietruszka, J. (2017) Synthesis and cytotoxic activities of goniothalamins and derivatives. *Bioorganic and Medicinal Chemistry*, **25(22)**, 6115–6125.

17. Blázquez, M. A., Bermejo, A., Zafra-Polo, M. C. and Cortes, D. (1999) Styryl-lactones from Goniothalamus species: A review. *Phytochemical Analysis*, **10(4)**, 161–170.

18. Mohd Ridzuan, M. A., Ruenruetai, U., Noor Rain, A., Khozirah, S. and Zakiah, I. (2006) Antimalarial properties of Goniothalamin in combination with chloroquine against Plasmodium yoelii and Plasmodium berghei growth in mice. *Tropical Biomedicine*, **23(2)**, 140–146.

19. Angelo, D. F., Kohn, L. K. and Pilli, R. A. (2006) Cytotoxic activity of (S)-goniothalamin and analogues against human cancer cells. *Biorganic and Medical Chemitry*, **14**, 622–631.

20. Asojo, O. A., Gulnik, S. V., Afonina, E., Yu, B., Ellman, J. A., Haque, T. S. and Silva, A. M. (2003) Novel uncomplexed and complexed structures of plasmepsin II, an aspartic protease from Plasmodium falciparum. *Journal of Molecular Biology*, **327(1)**, 173–181.

21. Friedman, R. and Caflisch, A. (2007) The proto-nation state of the catalytic aspartates in plasmepsin II. *FEBS Letters*, **581(21)**, 4120–4124.

22. Favre, A., Carreaux, F., Deligny, M. and Carboni, B. (2008) Stereoselective synthesis of (+)-goniodiol, (+)-goniotriol, (-)-goniofupyrone, and (+)-altholactone using a catalytic asymmetric hetero-Diels-Alder/allylboration approach. *European Journal of Organic Chemistry*, **29**, 4900–4907.

23. Tsubuki, M., Kanai, K., Nagase, H. and Honda, T. (1999) Stereocontrolled syntheses of novel styryl lactones, (+)-goniodiol, (+)- goniotriol, (+)-8-acetylgoniotriol, (+)-goniofufurone, (+)-9-deoxygoniopypyrone, (+)-goniopypyrone, and (+)-altholactone from common intermediates and cytotoxicity of their congener. *Tetrahedron*, **55(9)**, 2493–2514.

24. Dumitrescu, L., Huong, D. T. M., Hung, N. Van, Crousse, B. and Bonnet-Delpon, D. (2010) Synthesis and cytotoxic activity of fluorinated analogues of Goniothalamus lactones. Impact of fluorine on oxidative processes. *European Journal of Medicinal Chemistry*, **45(7)**, 3213–3218.

25. Chen, J., You, Z. and Qing, F. (2013) Total synthesis of g-trifluoromethylated analogs of goniothalamin and their derivatives. *Journal of Fluorine Chemistry*, **155**, 143–150.

26. Ramesh, P., Narasimha, Y., Narendar, T. and Srinivasu, N. (2017) Asymmetry First total synthesis of the highly potent antitumor lactones 8-chlorogoniodiol and parvistone A: Exploiting a bioinspired late-stage epoxide ring-opening. *Tetrahedron: Asymmetry*, **28(2)**, 246–249.

27. Kasaplar, P., Yilmazar, O. and Cagi, A. (2009) 6-Bicycloaryl substituted (S)- and (R)-5,6-dihydro-2H-pyran-2-ones: Asymmetric synthesis, and anti-proliferative properties. *Bioorganic & Medicinal Chemistry*, **17**, 311–318.

28. Zhou, F. S., Tang, W. D., Mu, Q., Yang, G. X.,

Wang, Y., Liang, G. L. and Lou, L. G. (2005) Semisynthesis and Antitumor Activities of New Styryl-Lactone Derivatives. *Chemical & Pharmaceutical Bulletin*, **53(11)**, 1387–1391.

29. Coura, R., Cezar, J., Caixeta, V., Vendraminicosta, D. B., Ernesto, J., Carvalho, D. and Aloise, R. (2012) Bioorganic & Medicinal Chemistry and their in vitro evaluation against human cancer cells. *Bioorganic & Medicinal Chemistry*, **20(11)**, 3635–3651.

30. Lipinski, C. A., Dominy, B. W. and Feeney, P. J. (1997) Experimental and computational approaches to estimate solubility and permeability in drug discovery and development settings. *Advanced Drug Delivery Reviews*, **23**, 3–25.

31. Lipinski, C. A., Lombardo, F., Dominy, B. W. and Feeney, P. J. (2012) Experimental and computational approaches to estimate solubility and permeability in drug discovery and development settings. *Advanced Drug Delivery Reviews*, **64**, 4–17.

32. Pires, D. E. V., Blundell, T. L. and Ascher, D. B. (2015) pkCSM: Predicting small-molecule pharmacokinetic and toxicity properties using graph-based signatures. *Journal of Medicinal Chemistry*, **58(9)**, 4066–4072.

33. Daina, A., Michielin, O. and Zoete, V. (2017) SwissADME: A free web tool to evaluate pharmacokinetics, drug-likeness and medicinal chemistry friendliness of small molecules. *Scientific Reports*, **7**, 1–13.

34. Onodera, K., Satou, K. and Hirota, H. (2007) Evaluations of molecular docking programs for virtual screening. *Journal of Chemical Information and Modeling*, **47(4)**, 1609–1618.

35. Warren, G. L., Andrews, C. W., Capelli, A. M., Clarke, B., LaLonde, J., Lambert, M. H. and Head, M. S. (2006) A critical assessment of docking programs and scoring functions. *Journal of Medicinal Chemistry*, **49(20)**, 5912–5931.

36. Rasina, D., Otikovs, M., Leitans, J., Recacha, R., Borysov, O. V., Kanepe-Lapsa, I. and Jirgensons, A. (2016) Fragment-Based Discovery of 2-Aminoquinazolin-4(3H)-ones As Novel Class Nonpeptidomimetic Inhibitors of the Plasmepsins I, II, and IV. *Journal of Medicinal Chemistry*, **59(1)**, 374–387.

37. Morozov, A. V. and Kortemme, T. (2005) Potential Functions for Hydrogen Bonds in Protein Structure Prediction and Design. *Advances in Protein Chemistry*, **72(05)**, 1–38.